Simulation of Propeller Runner for Cylindrical Basin of Gravitational Water Vortex Power Plant

Shankar Nath Pandey[1], Raj Kumar Chaulagain[1] ,Bimal Pandey[2]

[1,] Department of Automobile and Mechanical Engineering, Thapathali Campus, IOE, Tribhuvan University, Nepal

[2,] Department of Electrical Engineering, Pashchimanchal Campus, *IOE, Tribhuvan University, Nepal*

Abstract

The gravitational water vortex power plant is an emerging technology of power generation from water vortex in a small amount. It can generate electricity in a low head of range (0.7-2m). This system is very simple and requires less keep-up. This research aims to develop the propeller type runner which gives optimum efficiency and cylindrical basin suitable for this propeller runner in GWVPP. The research has been conducted by developing a new propeller runner and cylindrical basin considering the top surface open as the atmosphere. Blade angle, discharge hole diameter of the basin, the position of runner, and rpm are optimized on CFD-based optimization. After the CFD analysis, the optimum blade angle was 43°, exit hole diameter of this basin was found 175 mm which is 20% of the basin diameter. The optimum height was found 785mm which is 65.42% of the total height. And the efficiency of the optimized system was 23.639 % at 40 rpm.

Keywords : Gravitational water vortex power plant (GWVPP), Computational fluid dynamics (CFD), Propeller Runner, Open channel flow, Two-phase Modeling

1. Introduction

The world's population is growing rapidly resulting a continuous rise in energy consumption. One of the most popular forms of energy is electrical energy which hasn't produced enough to satisfy global demand. The majority of the 940 million people (13 percent of the world's population) who lack access to electricity reside in rural areas. Even if the availability of electricity has increased recently, it is still not enough. 660 million people would be without electricity in 2030, based on current trends[1].

As a result, increasing electricity output, particularly in rural regions, is critical. So it is necessary to develop a system that makes adequate and efficient use of the bulk of underutilized sites. Among many sources of

*Corresponding author
Email: a shankarpandey2052@gmail.com

electricity, hydropower is one of them which can generate electricity that can be utilized in isolated communities [2]. Pico hydropower is less than 5kw while micro hydropower ranges from 5kw to 100kw. So pico hydro is not economically viable and is difficult to integrate into the national grid, so it can be used in small communities off-grid. It is exceedingly expensive and difficult to access power transmission lines in remote communities in developing nations like Nepal where the geography is complex. It is quite challenging to access electricity because the settlements are dispersed throughout steep terrain.
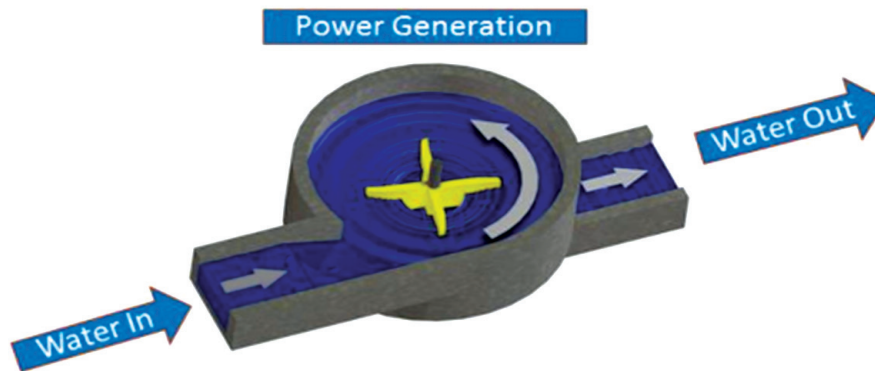
Figure 1: Gravitational vortex power plant[3]

A gravitational water vortex power plant utilizes renewable energy sources to produce electricity. In the vortex power plant, a free vortex is created by tangentially introducing water into a circular basin, and energy is then extracted from the free vortex using a turbine. A water vortex power plant operates differently from conventional hydroelectric facilities because it features a rotation tank with a central outlet where a stable vortex can form. Gravitational water vortex power plants are one of the most effective low-head power plants capable to runs between 0.7 and 2 meters [4]. As seen in Figure 1, the water in this plant enters by a sizable, straight intake and flows tangentially into a circular basin. The water will then create a strong vortex that emerges from the outflow in the shallow basin's center. At the center of the vortex, a vertical axis turbine extracts rotational energy from the gravitational vortex. The dynamic force of the vortex drives the turbine rather than a pressure differential. Small rivers and existing agricultural irrigation canals are examples of low-velocity water flow locations that are suited for this type of power generation system [4].

The technology behind the Gravitational Water Vortex Power Plant system is still in its development and is not yet fully developed. It is novel and developing to generate electricity from low-pressure water energy sources. The earlier research primarily concentrated on the analysis of various characteristics, such as the GWVPP canal length, the notch angle, the cone angle, and the basin shape, and optimizing these characteristics to obtain maximum efficiency [4].In addition, the turbine is the primary component and should be optimized for improved performance, so researchers are focusing on optimizing the runner. The main areas of focus for runner optimization are the tip-to-hub diameter ratio, blade profile, size and numbers of blade position of the runner, and blade inlet angle. The vortex power plant's optimization uses both experimental and numerical simulation methodologies.

Despite moving to a different sort of runner that would be more suited for a water vortex, many researchers have concentrated on adjusting runner twist angle and form in a previous study [4]. Numerous researchers in earlier studies take the top surface of GWVPP as a closed wall that is open to the atmosphere, and water is the only fluid that takes part in the system but in an open atmosphere air and water both influence the system[5] [6]. To remedy these drawbacks of past research, this research intended on developing a new type runner while taking into account top surface open as atmosphere and by using air and water both take part in simulation as two-phase modeling. Some related research and works have been conducted in gravitational water vortex, they provide some guidelines.The research conducted in GWVPP's cylindrical and conical basins by [7] discovered that the higher efficiency and power is developed by conical basin then cylindrical basin. Additionally, the maximum efficiency of 36.84% was found and maximum energy can be generated at a

height of 65-70% of the basin from the top surface. Numerical optimization of runner blade produced greatest efficiency of 12.08% by [8] in considering open channel flow.

In the research conducted by [9] different runner designs on CFD optimization with straight blade profile, twisted blade profile, and curved blade profiles, found that the blade having curved profile had a higher peak efficiency of 82.4% and straight blade profile gives efficiency of 46.31% and the twisted blade profile's 63.54%. According to research by [10] on the parameter that effects the performance of system was runner height and it is key point to be considered for designing of turbine runner. From the experiments, the greatest efficiency of 47.85% was found. While performing the research by [11] discovered that the conical basin produces powerful vortices than cylindrical basin. The results from [12] were supported by the finding that efficiency was highest in the lowest position. Greater efficiency is produced by fewer numbers of blades, whereas a loss in efficiency is produced by increasing the blade radius.

Water head of 0.12m developed a highest tangential velocity at free-vortex surface and turbine having three numbers of blade and having outer diameter of 0.027 m has produced highest efficiency of 43% in research conducted by [13].

2. Design Methodology

The design methodology for propeller runner and cylindrical basin involves following different steps.

2.1 Design of Propeller Runner

The head (H), volume flow rate (Q), power on shaft (P), and shaft speed is the first important design parameters for propellers. The design procedure suggested by [14] was adopted for the design of the propeller runner. For this, the head and power were assumed to be 1 m and 1 KW, respectively, and the necessary discharge was computed.

Discharge rate (Q) = $\frac{P}{\rho*g*h*\eta}$ [14]

= $0.1274 \ m^3/sec$

Once that specific speed has been determined

Specific speed $N_{S=\frac{2.294}{H^{0.486}}}$ [15]

After designing the head, specific speed, and power the speed of the shaft is calculated

Shaft speed (N) = $\frac{N_{SP}*(g*H)^{1.25}}{\sqrt{power \ avialable}}$ [14]

= $\frac{137.64*(9.81*1)^{1.25}}{\sqrt{1000}}$ = 75.57 rpm

This specific speed is within the range of a propeller turbine. The diameter of the runner is then determined using an empirical formula proposed by [15]

Diameter of runner $(D_{runner}) = 84.5(0.79 + 1.602 N_S)*\frac{\sqrt{H}}{60*\Omega}$

= 0.794 m

The diameter of the hub to the diameter of the tip is a prime concern for the design of the runner. So hub to tip ratio was taken as 0.42 [15] then the diameter of the hub was calculated as D_{hub} =0.333 m. Seven numbers of blades were calculated from the sizing sheet suggested by [14]. For blade shape and profile, the solidity ratio is a major concern [16]. The profile is generated by taking three points from hub to tip.

Solidity ratio = $\frac{Numner\ of\ blades*chord\ length}{\pi*turbine\ diameter}$ [16]

Therefore, the propeller's chord measures 176 mm, 296 mm, and 415 mm at its hub, middle, and tip, respectively. Prime design parameters were obtained in this way.

The main parameters to design a propeller runner are listed in Table 1.

Table 1: Parameters required to define Propeller runner

D_h:	Hub diameter
D_t:	Tip diameter
L:	length of the propeller
β:	Blade angle of a propeller
N:	Number of blades
H:	Height of the propeller
L_h:	Chord length at the hub side
L_t:	Chord length at the tip side
H_r:	Hub cap radius

From the above design data CAD modeling of propeller runner as shown in figure 2 was performed on SOLIDWORK. Different views of this initial proposed propeller runner are as shown in Figure 3.
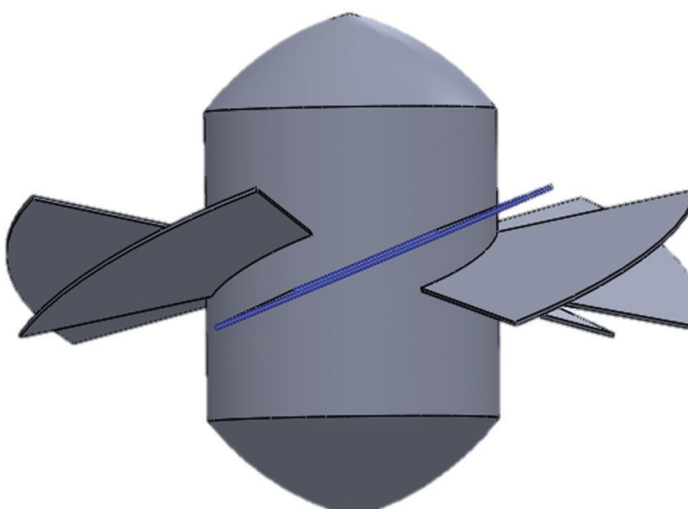
Figure 2: CAD modeling of proposed propeller runner
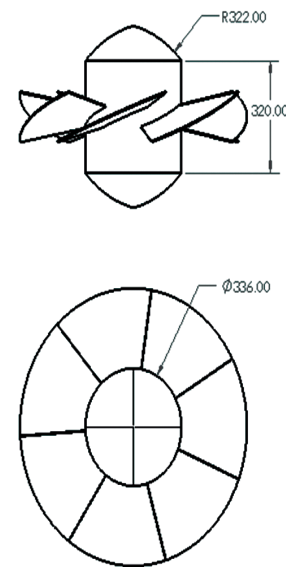
Figure 3: Different views of proposed propeller runner having blade angle 20º

2.2 Design of basin suitable for runner

While designing the basin, the diameter of the basin has been taken to 10% larger than the diameter of the propeller runner. The height of the basin was taken the 1200mm according to the height of the runner. The relation for cannel components such as cannel height, width, and length are referenced from [17]using a coaxial rotor with a vertical axis. The gravitational turbine has efficiencies that vary between 17 and 85%. Increasing the circulation was required in order to achieve the highest efficiency. The circulation is a function of some geometric parameters of the turbine, such as the ratios between the basin diameter (D_ and relations are as follows: cannel height/diameter of basin = 0.599, cannel width/diameter of basin = 0.2, and cannel length/diameter of basin = 0.5. So the cannel's parameters are 523 mm height, 175 mm width, and 437 mm length. The different views of cylindrical basin are as shown in figure 4.
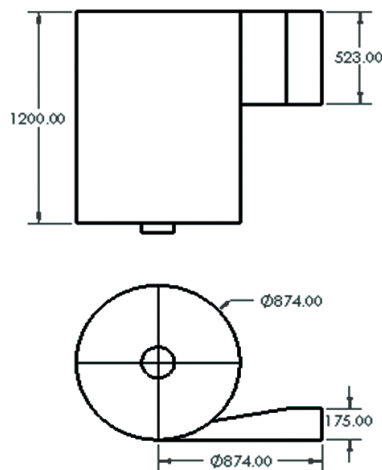
Fig 4: Different views of cylindrical Basin

2.3 Numerical Model Development

The discharge flow rate and torque developed by the runner at a specific angular velocity of the runner were calculated by numerical simulation. The power produced by the runner can be calculated once values for torque developed and discharge flow rate are known. Consequently, efficiency may be measured [2].

SOLIDWORKS was used as a CAD modeling program and ANSYS 2021 was used for numerical simulations. For CFD analysis, the SOLIDWORKS-produced CAD models were exported in STEP format and imported into ANSYS CFX. To improve the mesh quality and as a result, the accuracy of the solution, the mesh metrics such as skewness, orthogonal quality, element quality, etc. were tracked and maintained in an acceptable range. The model was split into the stationary domain for the basin and the rotational domain for the runner.

The governing equations are resolved using the finite volume method(FVM) in the commercial CFD software ANSYS CFX 2021. The governing equations incorporate the following contunity and momentum equation. [18] [9].

Continuity equation:

$$\frac{\partial \rho}{\partial t} + div(\rho u) = 0 \qquad (1)$$

Momentum equations:

$$\rho \frac{Du}{Dt} = \frac{\partial(-p + \tau_{xx})}{\partial x} + \frac{\partial \tau_{yx}}{\partial y} + \frac{\partial \tau_{zx}}{\partial z} + S_{Mx} \tag{2}$$

$$\rho \frac{Dv}{Dt} = \frac{\partial \tau_{xy}}{\partial x} + \frac{\partial(-p + \tau_{yy})}{\partial y} + \frac{\partial \tau_{zy}}{\partial z} + S_{My} \tag{3}$$

$$\rho \frac{Dw}{Dt} = \frac{\partial \tau_{xz}}{\partial x} + \frac{\partial \tau_{zy}}{\partial y} + \frac{\partial(-p + \tau_{zz})}{\partial z} + S_{Mz} \tag{4}$$

Where u, v, and w are the velocity components along the x, y, and z axis respectively, p is compressive stress, τ is tensile stress, S_M is the body forces, and $\frac{D}{Dt}$ is total derivative.

2.4 Physics Setup

Air and water were modeled in two phases for the analysis. This led to the employment of a multiphase Eulerian fluid method. The domain was set to have a temperature of 25° C and a reference pressure of 1 atm. The air density at 25 °C, 1.2 kg/m3, was chosen as the buoyancy reference density from [18]. The ANSYS software provided air and water properties were used. The analysis also took into account buoyancy because it is an important factor in the creation of air-core vortices. SST k-ω was the chosen turbulence model. Due to its ability to simulate air core vortices with greatly curved streamline flows, the SST k-ω model combines k-ω in the near-wall region and k-ω in the free streamline. Additionally, compared to the Reynolds Stress Model, it offers resilience with less computing time [6]. The boundary conditions for the CFD study of propeller runner in the cylindrical basin are mentoned in figure 5.

Opening
Boundry type: opening, Turbulence: medium, volume fraction: air =1, water=0
Opening pressure and direction with relative pressure 0 Pa

Interfaces
Type : Fluid Fluid
Model : General connection
Mixing Model : Frozen rotor
Pitch change option : Specified pitch
angle with angle side 360 degree

Inlet
Type : Inlet
Normal speed : 1.58 m/sec
Turbulence: medium (intensity 5%)
Volume fraction : water =1, air = 0

Wall
Boundry type: wall
No slip wall, Smooth walln

Outlet
Type : Outlet
Average static pressure with relative pressure

Figure 5: Boundary condition of the propeller runner system

2.5 Mesh Independency Test
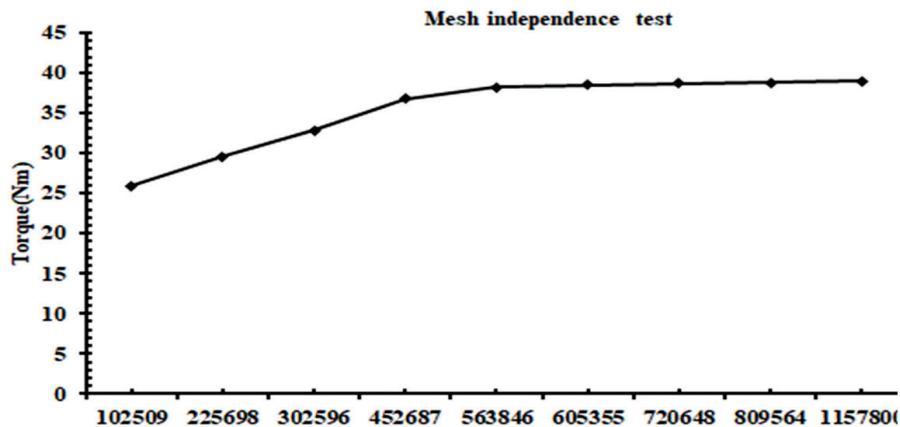
Figure 6: Mesh independence test of propeller runner

Nine different numbers of mesh elements with a range of 102509 to 1157800 were employed in the mesh independence test. On the runner, the torque was observed. Figure 6 depicts the graph that was drawn between the number of elements and the torque. The torque on a runner when elements 605355 is 38.558 Nm and torque on a runner when element 1157800 is 39.0175 Nm. So change in torque on these elements is 1.2 % which is acceptable. So 605355 elements were used for further processing.

3. Result and Discussion

Due to the top surface's exposure to the atmosphere in this scenario, not all of the water that was flowing through the intake struck the runner. In contrast to the closed top surface in single-phase flow of water, the outflow flow rate was not equal to the inlet flow rate. As a result, each simulation's discharge from the basin exit hole and torque was calculated using ANSYS code. Using these acquired values, the following equations were used to compute input and output power, and efficiency.

Power generated at runner = T*ω

Where,

T= Torque = torque y()@ runner Nm

ω = Angular velocity of the runner

ω = $\frac{2*\pi*N}{60}$ rad/sec

Input power = ρ*g*H*Q

Where,

ρ = density of water = 998 kg/m^3

g = Acceleration due to gravity = 9.81 m/s

H = head up to runner position

Q = Mass flow rate @outlet m^3/sec

Efficiency = $\frac{power\ generated\ at\ runner}{input\ power}$ * 100 %

3.1 Optimizing of Basin Exit Hole Diameter

For optimizing the basin outlet diameter, different CAD models of the basin having different outlet diameters were simulated at steady state conditions. The basin domain was stationary and the runner was rotating domain at 30 rpm. Torque on the runner was observed and outlet power is calculated. The outlet hole diameter at which the runner gives maximum torque is optimized outlet diameter. This process is conducted on 5 basins having different outlet diameters. From this analysis when the exit hole diameter is increased up to 0.175 m, the torque and power developed on the runner increase because of the formation of a strong water vortex. Increasing exit hole diameter beyond 0.175 m the torque and power gradually fall because of not the formation of a strong water vortex. So the optimum exit hole diameter for this propeller runner system is 0.175 m. And for further calculation, this optimum exit hole diameter was used. The water volume fraction contour of this basin having optimized outlet diameter is shown in figure 7. This figure shows the formation of air core in cylindrical basin. In top blue portion fraction of air is 1 so no water is available and in red portion the fraction of water is 1 so there is no air. In vortex, shown in middle that consists both air and water and value is as shown in legend. the figure 8 shows that torque and output power increases on increasing basin exit hole diameter upto 0.175 m and after that the value of torque and output power falls down.
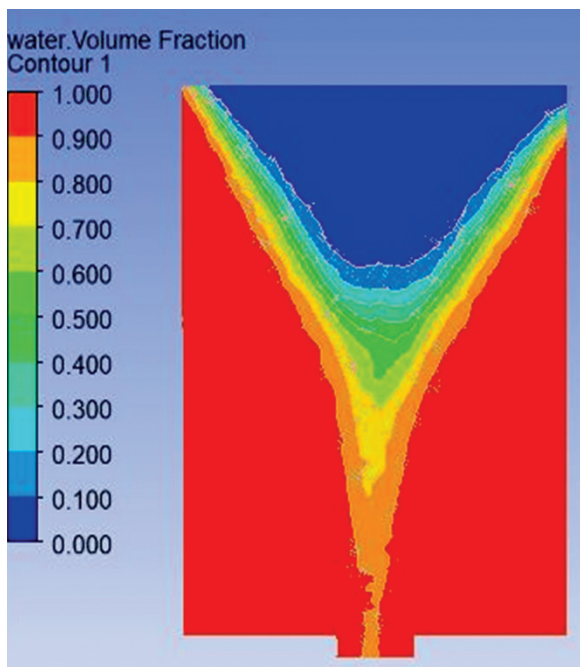
Figure 7: Water volume fraction contour of optimized basin
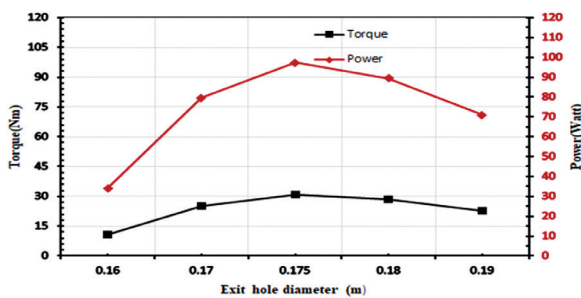
Figure 8: Variation of Torque and power with basin exit hole diameter

3.2 Optimizing the Blade angle of the propeller

For optimizing the propeller-type runner, fifteen different cad models of runners with various blade angles were simulated under steady state condition settings at 30 rpm. The result obtained from the simulation shows that torque, output power, and efficiency increase when the blade angle increases from 20° to 43°, and after that, these value gradually falls. The maximum torque of 38.144 Nm, the maximum output power of 119.833 Watt, and maximum efficiency of 20.633% were obtained. Similarly, the discharge and input power increases up to 44° and after that, these value also falls. The maximum discharge of 0.07415 and input power of 580.8381 Watt was obtained. So 43° blade angle is selected as the optimum blade angle. The water velocity streamlines in figure 9 and total pressure contour in figure 10 shows that water velocity increases when it enters the basin because of deflected angle on the channel and when the water streamline strikes the runner blade its velocity falls and has a maximum velocity at the outlet. And total pressure is maximum at the bottom outer side of the basin.
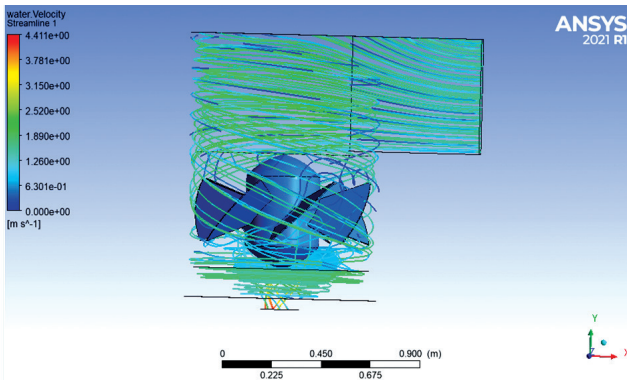
Figure 9: Water velocity streamlines
for optimized blade angle
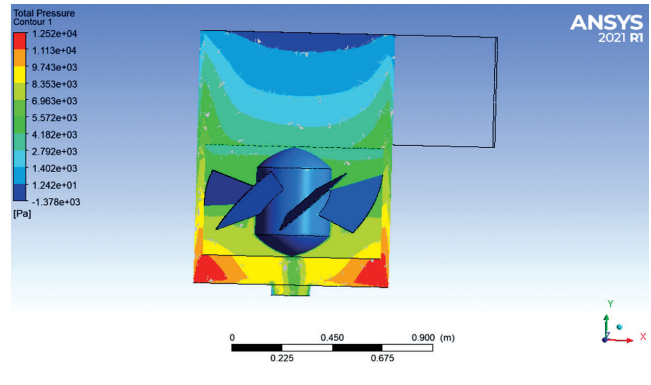
Figure 10: Total pressure contour of
optimized blade angle
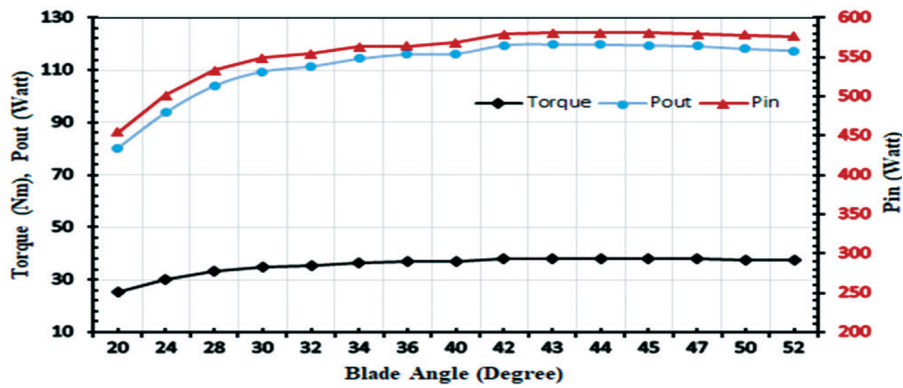
Figure 11: Variation of Torque, input, and output power with a blade angle of the propeller

Figure 11 shows the relation of torque, and power with blade angle of propeller runner. The torque and output power of propeller runner system increases upto blade angle of 43°and after that it falls down. And input power increases upto blade angle of 44° and after that it falls down.
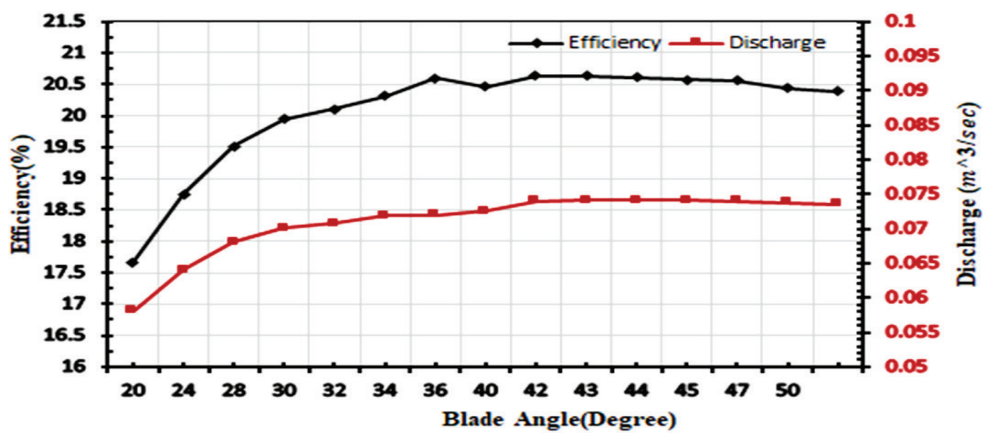
Figure 12: Variation of efficiency and discharge with a blade angle of the propeller

The efficiency increases while increasing blade angle from 20° to 43º and after that efficiency gradually falls down. Similarly, discharge is maximum at an blade angle of 44º as shown in figure 12.
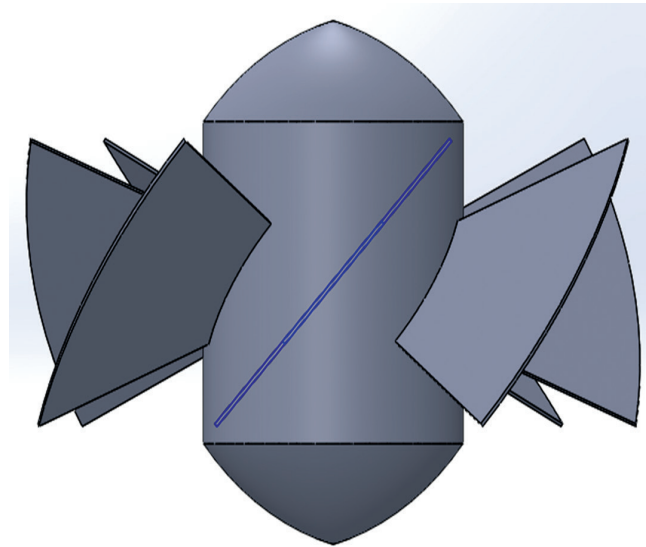
Figure 13: Optimized propeller runner having blade angle 43º

3.3 Optimizing the Position of Propeller

The position of the runner plays a crucial role in its efficiency because the vortex strength differs depending on the position. Therefore, five distinct cad models of the propeller runner system were built, each with a different position for the runner in the basin, for position optimization. The result obtained from the simulation shows that torque,output power, efficiency and discharge are maximum when runner is placed at top position of the basin which is the point where runner top point and cannel bottom point meets. After that torque, output power, efficiency and discharge gradually falls down as shown in figure 16 and figure 17. And maximum input power is required when runner is positioned at 0.816 m from top of basin. From the simulation, the maximum torque, output power, discharge, and efficiency are higher than the previous result obtained from the optimization of the runner only and the value is 38.874 Nm, 122.128 Watt, 0.0748 and 21.227 % respectively at a height of 0.785 m from the top of the basin. So the optimum position of the runner for this system is 0.785 m from the top of the basin. The water velocity streamline and total pressure contour of this system are shown in Figures 14 and figure 15.
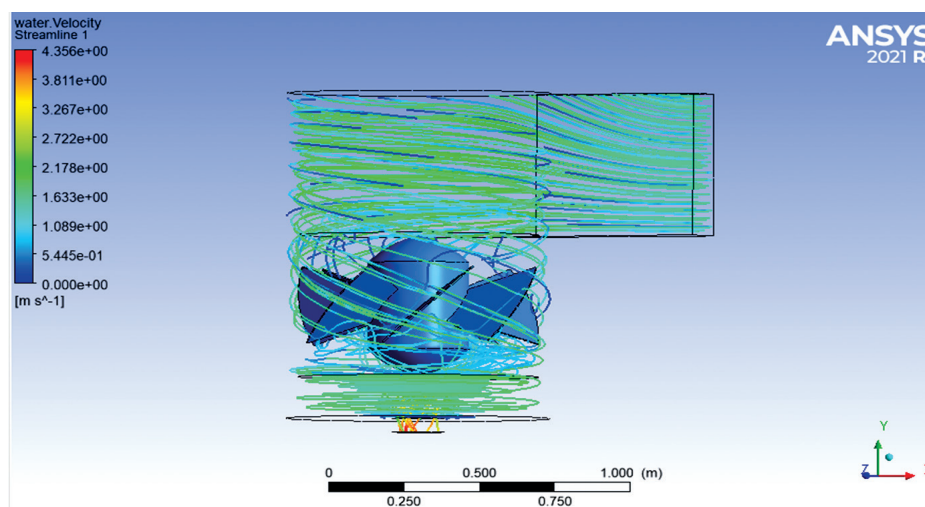
Figure 14: Water velocity streamlines of optimized position
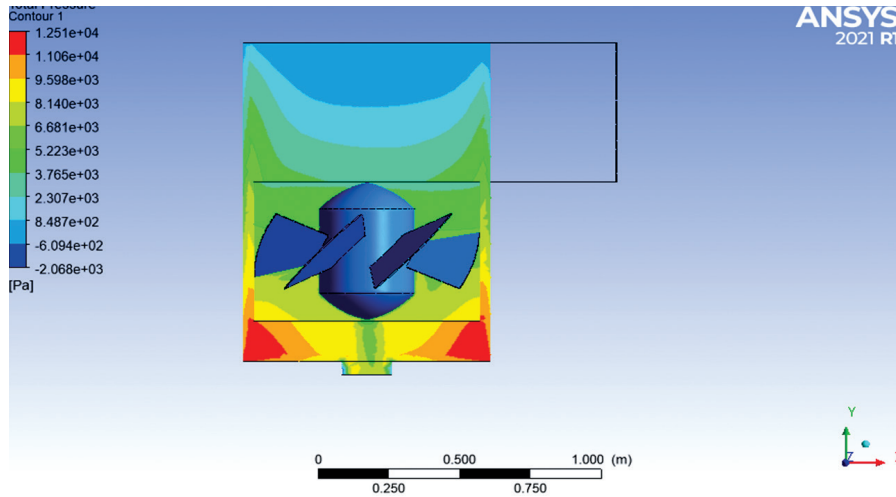
Figure 15: Total pressure contour of optimized position
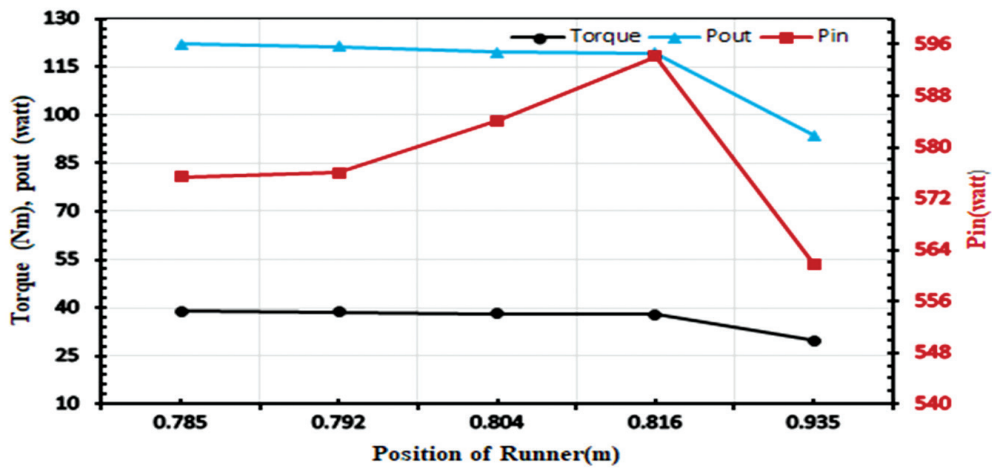
Figure 16: Variation of torque, input, and output power with the position of the runner
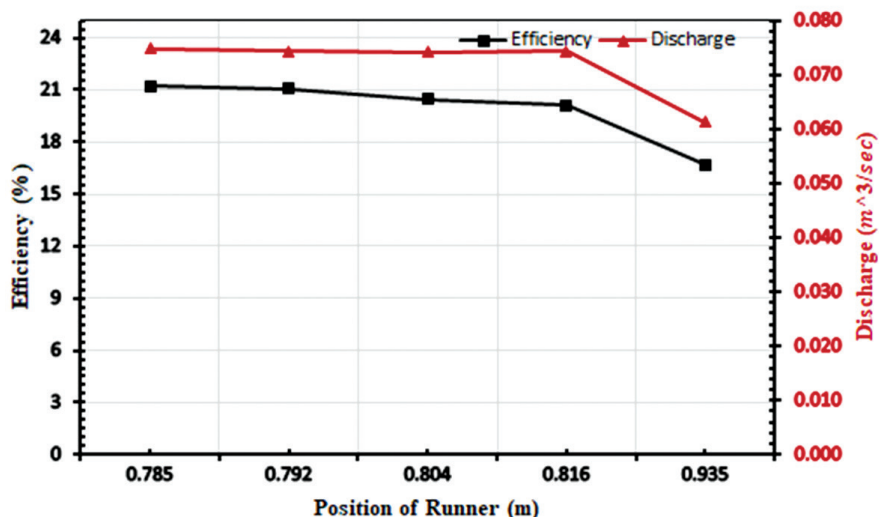
Figure 17: Variation of efficiency and Discharge with the position of the runner

97

3.4 Performance Analysis of Optimized Propeller Runner System

The steady state CFD analysis of the optimized propeller runner system has done at different speed to find out change in varialble with speed.. The water velocity streamlines in figure 18 and total pressure contour in figure 19 shows that water velocity is low when it enters in cannel and increases when water reaches the basin. When high-velocity water streamlines strike runner their velocity falls because of energy transfer and velocity again increase because of the exit hole diameter effect. The maximum velocity of the streamline is observed at the basin exit. Similarly, the total pressure of the system gradually increases as the height of the system increases. Maximum pressure is observed at the bottom outer side of the basin. A little negative pressure is observed at the outer surface of the basin exit hole, this indicates that efficiency can be further increased by the use of a draft tube.The relation of torque, power, efficiency and discharge with speed is shown in figure 20 and figure 21. This shows that torque, input power and discharge are maximum at 5 rpm and after that value of torque, input power, and discharge falls gradually. And the output power gradually increases upto 35 rpm and efficiency gradually increases upto 40 rpm and after that output power and efficiency fall down.

From result the maximum efficiency developed by propeller runner system was found 23.639% at 40 rpm. Where torque, power, and discharge are 27.43 Nm, 114.910 watts and 0.0634 respectively.
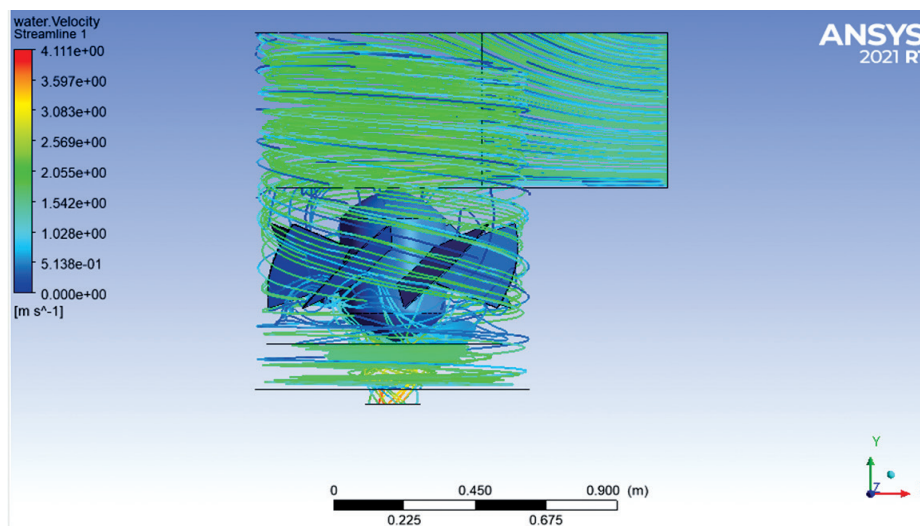
Figure 18: Water velocity streamlines of the optimized propeller runner system
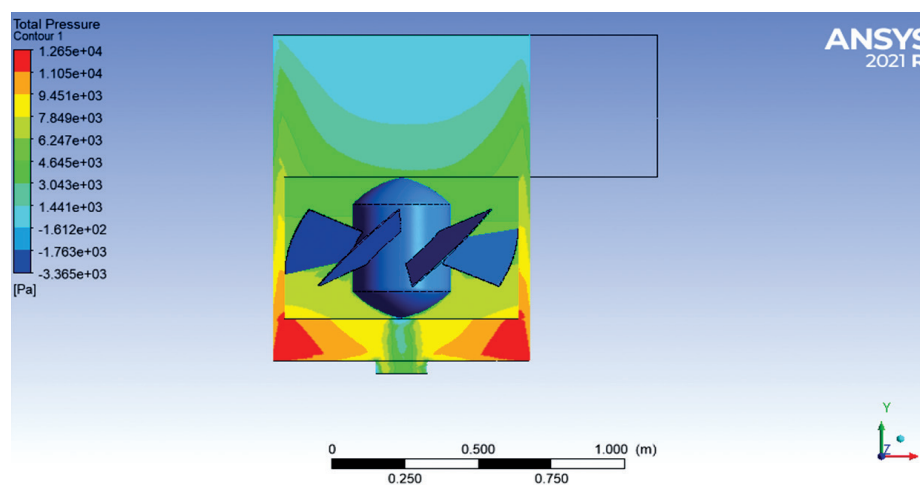
Figure 19: Total pressure contour of the optimized propeller runner system
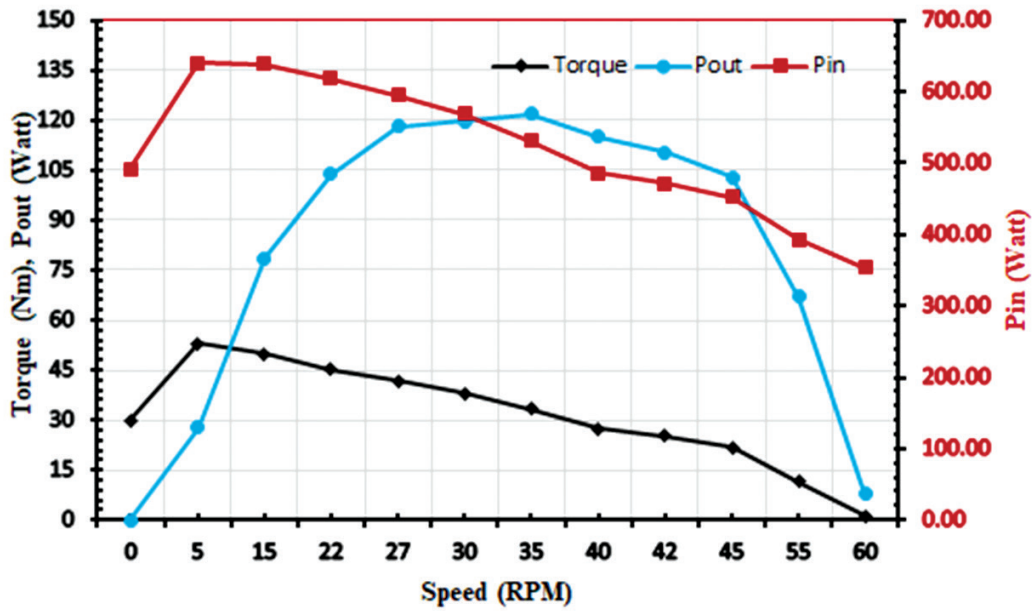
Figure 20: Variation of Torque, input, and output power with speed
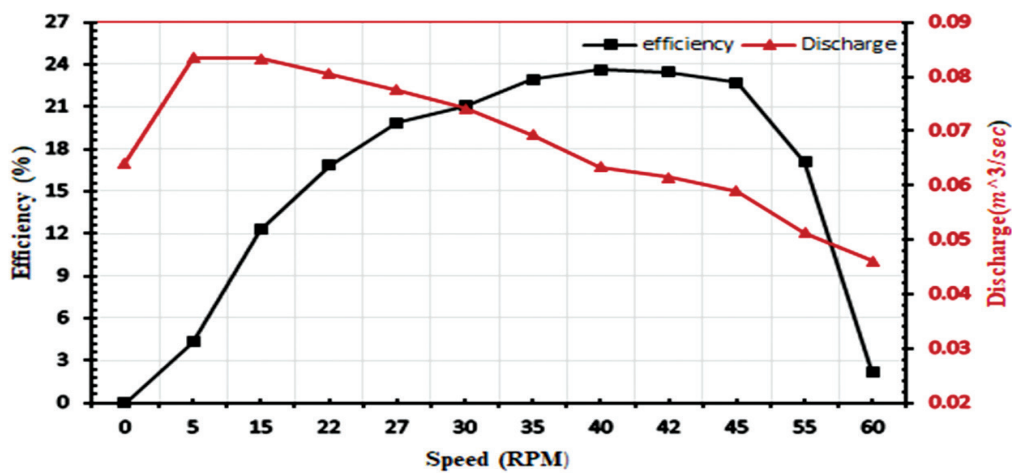
Figure 21: Variation of efficiency and discharge with speed

3.5 Mesh independence test of optimized propeller runner system
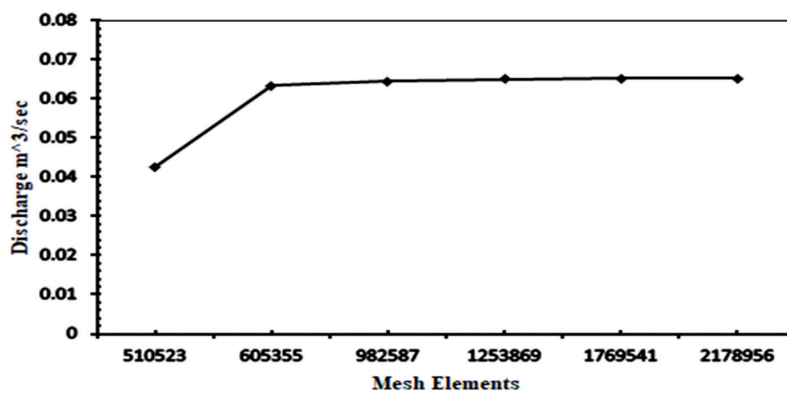
Figure 22: Mesh independence test of the optimized propeller runner system

Mesh independence test has been conducted by taking the discharge as a prime parameter obtained from the propeller runner system which is shown in figure 22. Different numbers of mesh element has been used for calculation ranging from 510523 to 2178956 and discharge has been obtained. The change in discharge was very low beyond the 605335 numbers of elements. When mesh elements 2178956 were used the discharge 0.06532   was obtained and when mesh element 605355 were used the discharge was 0.06343 . So the change in discharge was in range of 2.97% . Therefore the result by using 605355 numbers of element was very close to accuracy.

4. Conclusion

In this research, the propeller runner and cylindrical basin were designed. Different parameters of propeller runner systems like basin exit hole diameter, propeller runner blade angle, and position of a runner in a cylindrical basin are optimized by CFD analysis. From this research propeller runner system has optimum basin exit hole diameter is 175 mm and which is 20 % of basin diameter.The optimum blade angle of the propeller is 43° for this system and the optimum position of a runner in this system is 785 mm which is 65.42 % of the total height from the top of the basin. At this blade angle and position, maximum water streamline strikes the runner so maximum efficiency is found at 23.639 % with output power 114.910 watt at 40 rpm.

Further research on this study can be done by considering top surface close as a wall and considering water is only fluid influencing in the process like previous studies. Practical experiment can be done by building physical model and result obtained from simulation and experiment can be compared. The research can be further extend by adding draft tube to increase pressure head. Similarly this research can further extended to conical basin.

Acknowledgment

Conflict of interest

Not declared by the author(s).

References

[1]   I. D. and projections. Https: and //www.iea.org/reports/ Sdg7-data-and-projections, *IEA. Data Proj. https //www.iea.org/reports/ sdg7-data-and-projections, 2020. Accessed January 2, 2021.*, 2020.

[2]   A. Gautam, A. Sapkota, S. Neupane, J. Dhakal, A. B. Timilsina, and S. Shakya, "Study on Effect of Adding Booster Runner in Conical Basin : Gravitational Water Vortex Power Plant : A Numerical and Experimental Approach," *Proc. IOE Grad. Conf.*, pp. 107–113, 2016.

[3]   Dr. Gurmit Singh, "Gravitational Water Vortex 15 kW Mini Hydro Turbine," no. January 2019.

[4]   M. M. Rahman, J. H. Tan, M. T. Fadzlita, and A. R. Wan Khairul Muzammil, "A Review on the Development of Gravitational Water Vortex Power Plant as Alternative Renewable Energy Resources," *IOP Conf. Ser. Mater. Sci. Eng.*, vol. 217, no. 1, 2017, doi: 10.1088/1757-899X/217/1/012007.

[5]   N. Regmi, H. Bahadur Dura, S. Raj Shakya, and H. Dura, "Design and Analysis of Gravitational Water Vortex Basin and Runner Study on Conical Basin for Water Vortex Powerplant View project ALIEN Project View project Design and Analysis of Gravitational Water Vortex Basin and Runner," no. June

2020, 2019, [Online]. Available: conference.ioe.edu.np/publications/ioegc2019-winter/.

[6]   T. R. Bajracharya, Shree raj Shakya, Ashesh Babu Timilsina, Jhalak Dhakal, Subash Neupane, Ankit Gautam, and Anil Sapkota, "Effects of Geometrical Parameters in Gravitational Water Vortex Turbines with Conical Basin," vol. 2020, no. Figure 1, 2020.

[7]   S. Dhakal, Ashes B. Timilsins, Rabin Dhakal, Dinesh Fuyal, Tri Ratna Bajracharya, Hari P. Pandit, Nagendra Amatya, and Amrit Man Nakarmi, "Comparison of cylindrical and conical basins with the optimum position of runner: Gravitational water vortex power plant," *Renew. Sustain. Energy Rev.*, vol. 48, pp. 662–669, 2015, doi: 10.1016/j.rser.2015.04.030.

[8]   H. H. Khan, "Blade Optimization of Gravitational Water Vortex Turbine," *Ghulam Ishaq Khan Inst. Eng. Sci. Technol.*, vol. 6, no. 2, pp. 1689–1699, 2016, [Online]. Available: http://doi.wiley.com/10.1002/ ceas.12013%0Ahttps://www.researchgate.net/publication/317087330%0Ahttps://repositories.lib. utexas.edu/handle/2152/39127%0Ahttps://cris.brighton.ac.uk/ws/portalfiles/portal/4755978/ Julius+Ojebode%27s+Thesis.pdf%0Ausir.salford.a.

[9]   R. Dhakal, *T.R. Bajracharya, S.R Shakya, and B. Kumar*, "Runner for Gravitational Water Vortex Power Plant," *6th Int. Conf. Renew. Energy Res. Appl.*, vol. 5, pp. 365–373, 2017.

[10]   S. Dhakal, Sagar Dhakal , A. B. Timilsina , R. Dhakal , D. Fuyal , Tri Ratna Bajracharya , Hari Prasad Pandit "Effect of dominant parameters for conical basin gravitational water vortex power plant specification of the appropriate boundary conditions at cells which coincide with or touch the domain boundary .," *Proc. IOE Grad. Conf.*, no. February 2016, pp. 380–386, 2014, [Online]. Available: https:// www.researchgate.net/publication/280776139.

[11]   S. Dhakal, S. Nakarmi, P. Pun, A. B. Thapa, and T. R. Bajracharya, "Development and Testing of Runner and Conical Basin for Gravitational Water Vortex Power Plant," *J. Inst. Eng.*, vol. 10, no. 1, pp. 140–148, 2014, doi: 10.3126/jie.v10i1.10895.

[12]   M. G. Marian, T. Sajin, and A. Azzouz, "Study of micro hydropower plant operating in gravitational vortex flow mode," *Appl. Mech. Mater.*, vol. 371, pp. 601–605, 2013, doi: 10.4028/www.scientific.net/ AMM.371.601.

[13]   M. M. Rahman, T. J. Hong, R. Tang, L. L. Sung, F. Binti, and M. Tamiri, "Experimental Study the Effects of Water Pressure and Turbine Blade Lengths & Numbers on the Model Free Vortex Power Generation System," *Int. J. Curr. Trends Eng. Res.*, vol. 2, no. 9, pp. 13–17, 2016, [Online]. Available: http://www. ijcter.com.

[14]   R. Simpson and A. Williams, "Design of propeller turbines for pico hydro," pp. 1–15, 2011.

[15]   N. R. Prasad and S. J. Ranade, "Final Report of the HyPER Harvester Project Submitted by Partner with Southern New Mexico Elephant Butte Irrigation District (EBID) U . S . Department of Energy, Contract DE-EE0005411 Submitted to DOE Wind and Water Power Program," no. May 2012, 2015.

[16]   S. Joshi and A. K. Jha, "Computational and Experimental Study of the Effect of Solidity and Aspect Ratio of a Helical Turbine for Energy Generation in a Model Gravitational Water Vortex Power Plant," *J. Adv. Coll. Eng. Manag.*, vol. 6, pp. 213–219, 2021, doi: 10.3126/jacem.v6i0.38360.

[17]   L. Velásquez, A. Posada, and E. Chica, "Optimization of the basin and inlet channel of a gravitational water vortex hydraulic turbine using the response surface methodology," *Renew. Energy*, vol. 187, pp. 508–521, 2022, doi: 10.1016/j.renene.2022.01.113.

[18]   N. Regmi, H. Dura, and S. S. Raj, "Design and analysis of gravitational water vortex basin and runner," *IOP Grad. Conf.*, no. December 2019, pp. 157–164, 2020.